

# Spin-polarized Andreev molecules and anomalous nonlocal Josephson effects in altermagnetic junctions

Sayan Mondal and Jorge Cayao

*Department of Physics and Astronomy, Uppsala University, Box 516, S-751 20 Uppsala, Sweden*

(Dated: March 6, 2026)

Altermagnetism has emerged as a promising ingredient for realizing nontrivial Josephson phases but so far explored in single Josephson junctions. In this work, we consider the coherent coupling of two Josephson junctions with spin-singlet  $s$ -wave superconductivity and demonstrate that  $d$ -wave altermagnetism gives rise to spin-polarized Andreev molecules due to the hybridization of Andreev bound states of each junction when the coupling is weak. Interestingly, these spin-polarized Andreev molecules induce anomalous nonlocal Josephson effect, where the current flow across one Josephson junction due to phase changes across the other junction develops  $0 - \pi$  and  $\phi_0$  transitions originating from altermagnetism. Furthermore, the nonlocal Josephson current carried by spin-polarized Andreev molecules exhibits nonreciprocal critical currents, enabling a nonlocal Josephson diode effect whose polarity is tunable by the altermagnetic strength and right phase. Our findings put forward altermagnetism as a promising arena for designing nonlocal spin Josephson phenomena.

The advent of altermagnetism has provided a new front in the search of nontrivial superconducting phenomena that are promising for quantum applications [1, 2]. This is because altermagnets (AMs) possess anisotropic spin polarized Fermi surfaces and zero net magnetization [3–13], originated from a collinear-compensated magnetic ordering in real space that preserves inversion symmetry but breaks time-reversal symmetry. While these properties enabled the prediction of a number of unusual superconducting phases [1, 2, 14], their role on Josephson systems is of particular relevance because Josephson junctions (JJs) form the basis for superconducting electronics and quantum computing [15–29]. In this regard, AMs in single JJs have already proven crucial for inducing spin-polarized Andreev bound states (ABSs) [30–33], anomalous supercurrents [30, 32, 34–40], and nonreciprocal critical currents [41–47]. These advances show the potential of altermagnetism in single JJs, and naturally make us wonder about the impact of altermagnetism on coherently coupled JJs.

The coherent coupling of JJs has already inspired several theoretical [48–62] and experimental [63–74] efforts. Central to these works is the formation of Andreev molecules due to the hybridization of ABSs when coupling two JJs [48], a phenomenon tunable by the superconducting phase differences across each JJ. Andreev molecules form similarly to how natural atoms bond to form chemical molecules but based on the Andreev and Josephson physics. A unique property of the Andreev molecular regime is that the supercurrent flow across one JJ can be manipulated by the phase difference across the other JJ, enabling the so-called nonlocal JE [48]. At present, there already exists experimental evidence of Andreev molecules and of the nonlocal JE, thus supporting coherently coupled JJs for creating fundamental states and intriguing material properties. Despite this progress, however, the research on Andreev molecules and nonlocal JE has mainly focused on superconductor-

semiconductor systems, leaving seldom studied the role of the recently discovered altermagnetism.

In this work, we consider three coupled spin-singlet  $s$ -wave superconductors with  $d$ -wave altermagnetism and demonstrate the formation of spin-polarized Andreev molecules when spin-polarized ABSs of each JJ hybridize across the middle superconductor. Notably, we find that the spin-polarized Andreev molecules enable a anomalous phase-biased nonlocal Josephson effects, whereby a phase difference across one junction induces a supercurrent through the other. Depending on the altermagnetic crystal symmetries and strength of altermagnetism, the nonlocal Josephson current develops tunable transitions between  $0$ -,  $\pi$ -, and  $\phi_0$ -junction behaviors. We also show that the nonlocal supercurrents carried by spin-polarized Andreev molecules develop a nonreciprocal behavior, thereby signalling the emergence of a nonlocal Josephson diode effect. We find that the efficiency and polarity of this diode effect exhibit a strong tunability by the type and strength of altermagnetism. Our work establishes the interplay between altermagnetism and coherently coupled JJs as an outstanding ground for designing nonlocal Josephson phases with spin functionalities.

*Coupled JJs with altermagnetism.*—We consider the coherent coupling of two JJs with  $d$ -wave altermagnetism, where two spin-singlet  $s$ -wave superconductors are coupled through a spin-singlet  $s$ -wave superconductor [Figs. 1(a,f)]. The coupled JJs is assumed to be finite along  $x$  and periodic along the  $y$ , and modelled by

$$\mathcal{H}_{k_y}(\phi_L, \phi_M, \phi_R) = \sum_{\alpha} H_{k_y}(\phi_{\alpha}) + H_{LM} + H_{MR}, \quad (1)$$

where

$$\begin{aligned} H_{k_y}(\phi_{\alpha}) = & \sum_i c_i^{\dagger} h_{ii}(k_y) c_i + \sum_{\langle i,j \rangle} c_i^{\dagger} v_{ij}(k_y) c_j \\ & + \sum_i \Delta_{\alpha} (c_{i\alpha,\uparrow}^{\dagger} c_{i\alpha,\downarrow}^{\dagger} - c_{i\alpha,\downarrow}^{\dagger} c_{i\alpha,\uparrow}^{\dagger}) + \text{h.c.}, \end{aligned} \quad (2)$$

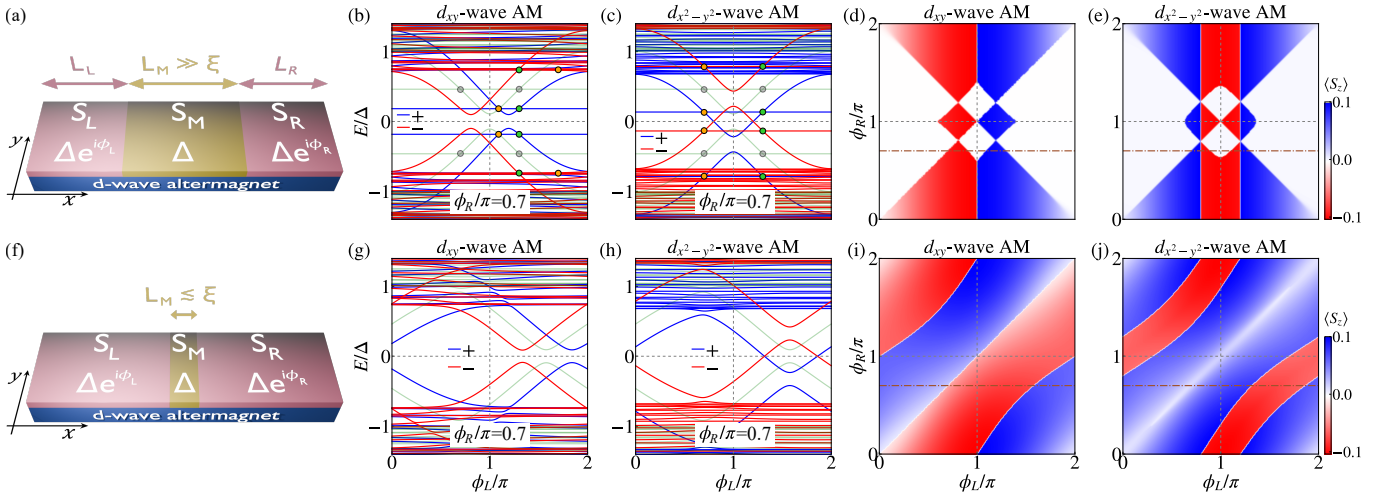


FIG. 1. (a,f) Sketch of the studied Josephson setup, where three spin-singlet  $s$ -wave superconductors denoted by  $S_\alpha$  ( $\alpha = L, R$  pink and  $\alpha = M$  gold) are in contact with a  $d$ -wave altermagnet (blue); the superconductors have lengths  $L_\alpha$  and pair potentials  $\Delta_\alpha = \Delta e^{i\phi_\alpha}$ , with  $\phi_M = 0$ . (a) and (f) correspond to  $S_M$  with a long ( $L_M = 100a \gg \xi$ ) and short ( $L_M = 2a \lesssim \xi$ ) length, where  $\xi$  is the superconducting coherence length and  $a$  is the lattice spacing. (b,c) Low-energy spectrum as a function of  $\phi_L$  at  $\phi_R = 0.7\pi$  and  $k_y = 0.1\pi$  for  $L_M \gg \xi$ , while (g,h) for  $L_M \lesssim \xi$ . The blue (red) color in (b,c,g,h) indicates that such energy levels belong to the Nambu sector formed by spin- $\uparrow$  electrons (holes) with spin- $\downarrow$  holes (electrons), denoted by ‘+’ (‘-’). The light green curves are the energy levels without altermagnetism. The filled yellow and green circles mark the positions where dispersionless levels of the right JJ cross with the dispersive levels of the left JJ in presence of the AM, while the filled gray circles mark the same but in absence of the AM. (d,e) Spin projection along  $z$  in the left JJ at  $k_y = 0.1\pi$  for  $L_M \gg \xi$ , while (i,j) for  $L_M \lesssim \xi$ . Parameters:  $L_L = L_R = 100a$ ,  $\mu = 1.5t$ ,  $\Delta = 0.2t$ ,  $\phi_M = 0$ .

describes the left (L), middle (M), and right (R) superconductor ( $\alpha = L, M, R$ ) with  $d$ -wave altermagnetism. Here  $c_i = (c_{i,\uparrow}, c_{i,\downarrow})^T$ , where  $c_{i,\uparrow}$  annihilates an electronic state with spin  $\sigma = \uparrow, \downarrow$  at  $i$ . Moreover,  $h_{ii}(k_y) = [-\mu + 4t - 2t \cos k_y] \sigma_0 - J_2 \cos k_y \sigma_z$  and  $v_{ij}(k_y) = -t\sigma_0 - iJ_1 \sin k_y \sigma_z + (J_2/2)\sigma_z$  correspond to onsite and nearest neighbor terms, which are block diagonal in spin space,  $\sigma_i$  are the spin Pauli matrices,  $t$  denotes the hopping strength,  $\mu$  the chemical potential, while  $J_1$  and  $J_2$  represent the strength of the  $d_{xy}$ - and  $d_{x^2-y^2}$ -wave altermagnetism. Furthermore,  $\Delta_\alpha = \Delta e^{i\phi_\alpha}$  is the pair potential in  $\alpha$  superconductor; by gauge symmetry [62], we set  $\phi_M = 0$  and keep  $\phi_{L,R} \neq 0$  characterizing the superconducting phase differences across the left and right JJs. The term  $H_{LM(MR)}$  couples the left and middle (middle and right) superconductors, having non-zero values only between the sites adjacent to the interfaces. Next we denote  $\mathcal{H}_{k_y}(\phi_L, \phi_R) \equiv \mathcal{H}_{k_y}(\phi_L, \phi_M = 0, \phi_R)$ .

Before going further, we discuss the symmetries of the JJ setup in Eq. (1). Without the AM, the JJ Hamiltonian preserves global time-reversal symmetry (TRS),  $\mathcal{T}\mathcal{H}(\phi_L, \phi_R)\mathcal{T}^{-1} = \mathcal{H}(-\phi_L, -\phi_R)$ , but local TRS can be broken  $\mathcal{T}\mathcal{H}(\phi_L, \phi_R)\mathcal{T}^{-1} \neq \mathcal{H}(-\phi_L, \phi_R)$ , where  $\mathcal{T}$  denotes the time-reversal operator. In the presence of an AM, global TRS is broken. In addition, in the presence and absence of AM, the JJ intrinsically breaks local spatial inversion,  $\mathcal{I}\mathcal{H}(\phi_L, \phi_R)\mathcal{I}^{-1} \neq \mathcal{H}(-\phi_L, \phi_R)$ , with  $\mathcal{I}$  the inversion operator. Thus, breaking local time-reversal and local inversion symmetries is very likely to lead to unusual

ABSs and supercurrents; in fact, the simultaneous breaking of these symmetries satisfies the necessary conditions for the Josephson diode effect [75–85], suggesting that our JJ in Eq. (1) can host intriguing Josephson physics.

*Spin-polarized Andreev molecules.*—We begin by inspecting the role of the superconducting phase differences  $\phi_{L,R}$  on the low-energy spectrum of our coupled JJs with altermagnetism [Eq. (1)]. For this reason, Figs. 1(b,c) show the low-energy spectrum as a function of  $\phi_L$  with  $d_{x^2-y^2}$ - and  $d_{xy}$ -wave altermagnetism, in both cases  $\phi_R = 0.7\pi$ ,  $k_y = 0.1\pi$  for a middle superconductor longer than the superconducting coherence length  $\xi$  ( $L_M \gg \xi$ ). To contrast this regime, Figs. 1(g,h) show the low-energy spectrum for a short middle superconductor ( $L_M \lesssim \xi$ ). These short and long middle superconductor regimes capture the weak and strong couplings between JJs. To complement the analysis in these two regimes, Figs. 1(d,e,i,j) shows the spin polarization  $\langle S_z \rangle$  in the left JJ for the first positive ABS. In the absence of altermagnetism, the left (right) JJ host four spin-degenerate ABSs that depend on  $\phi_{L,R}$  and  $L_M$ , with a  $2\pi$ -periodic energy spectrum that is symmetric about  $\phi_L = \pi$ , see light green curves in Figs. 1(b,c,g,h). For  $L_M \gg \xi$ , the left and right JJs behave as independent [Figs. 1(b,c)]: the ABSs of the left JJ exhibit a strong dependence on  $\phi_L$ , while those ABSs of the right JJ remain dispersionless and intersect the ABSs of the left JJ at  $\phi_R = \phi_L$ , as indicated by the gray circles in Fig. 1(b). In contrast, for  $L_M \lesssim \xi$  [Figs. 1(g,h)], the ABSs of both junctions hybridize, leav-

ing only a single pair of hybridized ABSs that strongly disperses with  $\phi_{L,R}$  and is asymmetric with respect to  $\phi_L = \pi$ . The dependence of the hybridized ABSs on  $L_M$  resembles an interatomic potential describing molecular formation, giving rise to the so-called Andreev molecules [48]; see Fig. 5 in E2 of the End Matter.

With altermagnetism, the low-energy spectrum develops interesting changes in short and long middle superconductors, see Figs. 1(b,c,g,h). First, a finite amount of altermagnetism makes ABSs to split in spin, giving rise to spin-polarized ABSs with a behavior that strongly depends on the ratio between  $L_M$  and  $\xi$  as well as on the type of altermagnetism and  $\phi_{L,R}$ . For  $L_M \gg \xi$ , only the spin-polarized ABSs of the left JJ disperse with  $\phi_L$ , while the spin-polarized ABSs of the right JJ remain dispersionless and intersect those ABSs of the left JJ at  $\phi_R = \phi_L$ ; owing to the  $2\pi$  periodicity of the spectrum, a similar intersection occurs at  $\phi_R = 2\pi - \phi_L$ , see Figs. 1(b,c) and yellow/green circles. The fact that ABS of the left JJ disperse only with  $\phi_L$  and the ones of the right JJ remain dispersionless occurs because the left and right JJs are weakly coupled due to  $L_M \gg \xi$ . Interestingly, while  $d_{xy}$ -wave altermagnetism splits ABSs shifting them to distinct minima above and below  $\phi_L = \pi$ ,  $d_{x^2-y^2}$ -wave altermagnetism splits ABSs to higher and lower energies but maintaining the same minimum at  $\phi = \pi$ . This dependence in  $d_{x^2-y^2}$ -wave AMs, makes ABSs to reach and cross zero energy, as in Fig. 1(c). Moreover, the finite size of the setup naturally induces a quasicontinuum, where, depending on the strength and type of altermagnetism, the spin-polarized ABSs can leak and/or touch the gap edges; for instance, under  $d_{xy}$ -wave altermagnetism, ABSs with distinct spin polarization touch the gap edges at  $\phi_L = 0, 2\pi$ , while ABSs of the same polarization reach the gap edges at  $\phi_L = 0, 2\pi$  with  $d_{x^2-y^2}$ -wave altermagnetism. Despite these differences between altermagnetic symmetries at  $L_M \gg \xi$ , the energy spectrum is symmetric about  $\phi_L = \pi$  for any  $\phi_R$ .

When the middle superconductor is very short ( $L_M \lesssim \xi$ ), the spin-polarized ABSs of the left and right JJs undergo a strong hybridization that gives rise to spin-polarized Andreev molecules; see Figs. 1(g,h). These spin-polarized Andreev molecules now constitute the sub-gap states of the strongly coupled JJs, and are, therefore, extremely sensible to variations of  $\phi_{L,R}$ . In fact,  $d_{xy}$ -wave altermagnetism splits the hybridized ABSs into spin-polarized Andreev molecules along  $\phi_L$ , developing minima below and above  $\phi_L^*$  [Figs. 1(g)], with  $\phi_L^*$  being the value of  $\phi_L$  at which the Andreev molecule has a minimum without altermagnetism. This behavior enables JJs with  $d_{xy}$ -wave AMs to host Andreev molecules with distinct polarizations at the same energies with a behavior that is asymmetric about  $\phi_L = \pi$ . For  $d_{x^2-y^2}$ -wave altermagnetism, the spin-polarized Andreev molecules are asymmetric about  $\phi_L = \pi$  and shifted in energy at  $\phi_L^*$ ; depending on the altermagnetic strength, they can reach

and cross zero energy; see Fig. 1(h). This leaves spin-polarized Andreev molecules with distinct spin polarizations crossing zero energy and at higher energies. The zero-energy crossings of the Andreev molecules are robust unless fields that couple distinct spins are applied. It is worth noting that the hybridized ABSs also leak into the quasicontinuum, but with subtle differences in each altermagnetic symmetry: the quasicontinuum of the JJ with  $d_{xy}$ -wave altermagnetism is composed of mixed levels having the same and distinct polarizations, which implies that the spin-polarized Andreev molecule leaking into such quasicontinuum also hybridizes with the quasicontinuum levels of the same polarization [Fig. 1(g)]. In contrast, the quasicontinuum of the JJ with  $d_{x^2-y^2}$ -wave altermagnetism contains spin-polarized subsets at distinct energies, which ensures that the spin-polarized Andreev molecules leaking into the quasicontinuum do not hybridize with the quasicontinuum levels [Fig. 1(h)].

The spin-polarized nature is also supported by the behavior of the spin polarization  $\langle S_z \rangle$ , which we obtain in the left JJ and show in Figs. 1(d,e,i,j) as a function of  $\phi_{L,R}$  at  $k_y \neq 0$ . Figs. 1(d,e) show that  $\langle S_z \rangle$  for  $L_M \gg \xi$  behaves as an odd function of  $\phi_L$  for the  $d_{xy}$ -wave AMs ( $\langle S_z(\phi_L) \rangle = -\langle S_z(-\phi_L) \rangle$ ), whereas it behaves as an even function for the  $d_{x^2-y^2}$ -wave AMs ( $\langle S_z(\phi_L) \rangle = \langle S_z(-\phi_L) \rangle$ ). By close inspection, the profile of  $\langle S_z \rangle$  aligns well with the spin-polarized nature of the ABSs shown in Figs. 1(b,c), see dash-dotted line in Figs. 1(d,e). In contrast, for  $L_M \lesssim \xi$ ,  $\langle S_z \rangle$  acquires a distinct behavior that reflects opposite spin polarization along  $\phi_L = \phi_R$ : this implies that  $\langle S_z(\phi_L, \phi_R) \rangle = \pm \langle S_z(-\phi_L, -\phi_R) \rangle$  for the JJs with  $d_{xy}$ - and  $d_{x^2-y^2}$ -wave altermagnetism, reflecting the key role of  $\phi_R$ . Still,  $\langle S_z \rangle$  determines the spin polarization of the emergent Andreev molecules. Thus, Figs. 1(d,e,i,j) not only support the spin polarized nature of Andreev molecules but also demonstrate the nonlocal phase control of spin polarization in coupled JJs.

*Anomalous nonlocal Josephson currents.*—Having shown the emergence of spin-polarized Andreev molecules, we now focus on the phase-biased Josephson current flowing across the left JJ, obtained for each  $k_y$  as  $I_L(k_y, \phi_L, \phi_R) = (e/\hbar) \sum_{E_n < 0} \partial E_n(k_y, \phi_L, \phi_R) / \partial \phi_L$  [29, 86, 87], this provides a way to pinpoint the contributions of distinct energy levels [88–94]. The total Josephson current flowing across the left JJ is then found as  $\mathcal{I}_L(\phi_L, \phi_R) = \int I_L(k_y, \phi_L, \phi_R) dk_y$ , which accounts for the weight of all transverse channels [1]. With this, in Fig. 2 we show  $\mathcal{I}_L(\phi_L, \phi_R)$  as a function of  $\phi_{L,R}$  in the presence of  $d_{x^2-y^2}$ -wave altermagnetism for long ( $L_M \gg \xi$ ) and short ( $L_M \lesssim \xi$ ) middle superconductors; for  $d_{xy}$ -wave altermagnetism, see E4 and Fig. 6 in the End Matter. When  $L_M \gg \xi$ , the current  $\mathcal{I}_L(\phi_L, \phi_R)$  is an odd function and  $2\pi$ -periodic with respect to  $\phi_L$  but insensitive to  $\phi_R$ , namely,  $\mathcal{I}_L(\phi_L, \phi_R) = -\mathcal{I}_L(-\phi_L, \phi_R)$  and  $\mathcal{I}_L(2\pi + \phi_L, \phi_R) = \mathcal{I}_L(\phi_L, \phi_R)$  [Fig. 2(a)]; these dependences also appear in regular JJs [95]. This is an

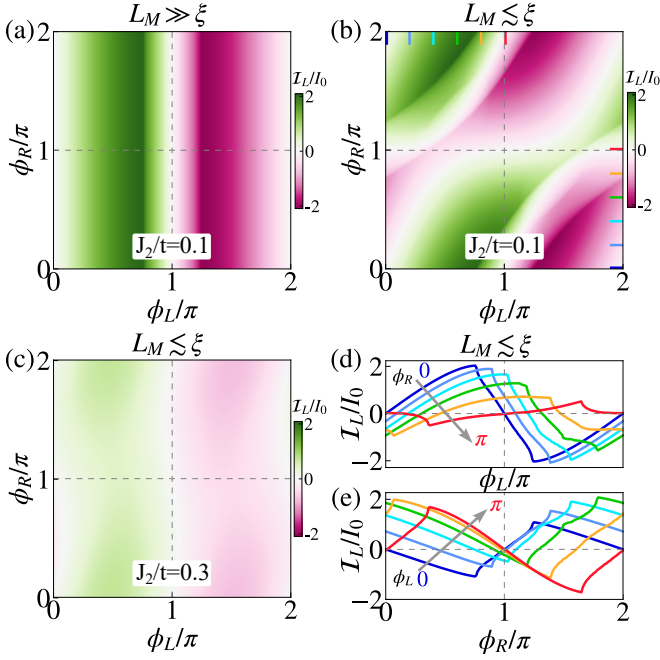


FIG. 2. Josephson current  $\mathcal{I}_L$  across the left JJ as a function of  $\phi_{L,R}$  in the presence of  $d_{x^2-y^2}$ -wave altermagnetism. (a)  $\mathcal{I}_L$  for  $L_M = 100a \gg \xi$  and  $J_2/t = 0.1$ , while (b,c) for  $L_M = 2a \lesssim \xi$  and  $J_2/t = \{0.1, 0.3\}$ . (d,e) Line cuts of  $\mathcal{I}_L$  in (b) as a function of  $\phi_{L(R)}$  at distinct  $\phi_{R(L)}$  in steps of  $0.2\pi$  marked by color bars in (b). Rest of parameters same as in Fig. 1

expected behavior consistent with the ABSs in Fig. 1(c) since the left and right JJs are effectively uncoupled and the spin-polarized ABS of the right JJ along with  $\phi_R$  do not affect the properties of the left JJ.

When  $L_M \lesssim \xi$ , the hybridization of spin-polarized ABSs that leads to spin-polarized Andreev molecules strongly affect the phase dependence of the  $\mathcal{I}_L(\phi_L, \phi_R)$ , see Fig. 2(b-d). In particular,  $\mathcal{I}_L(\phi_L, \phi_R)$  is now strongly dependent on  $\phi_R$ , developing negative/positive values for  $\phi_L < \pi$  and  $\phi_L > \pi$ , which depend on the strength of altermagnetism and are achieved after passing through zero values in both types of the studied AMs; see Figs. 2(b,c) and Figs. 6(b,c). Interestingly,  $\mathcal{I}_L(\phi_L, \phi_R) \neq 0$  at  $\phi_L = n\pi$ , with  $n \in \mathbb{Z}$ , and its oddness is now reflected by the simultaneous action of both phases  $\phi_{L,R}$  as  $\mathcal{I}_L(\phi_L, \phi_R) = -\mathcal{I}_L(-\phi_L, -\phi_R)$ ; this occurs in  $d_{x^2-y^2}$ - and  $d_{xy}$ -wave altermagnetism, see Figs. 2(b,c) and Figs. 6(b,c). As consequence of these properties is that the current flowing across the left junction develops  $\phi_0$ - and  $\pi$ -junction behaviors, either as a function of  $\phi_L$  or  $\phi_R$ , see Figs. 2(d,e). It is thus possible to have  $\mathcal{I}_L(\phi_L = 0, \phi_R \neq 0) \neq 0$  or  $\mathcal{I}_L(\phi_L + \pi, \phi_R) = -\mathcal{I}_L(\phi_L, \phi_R)$  for a  $\phi_{L0}$ -junction or  $\pi$ -junction, respectively. JJs with  $d_{xy}$ -wave altermagnetism can also host similar JJ profiles, see Figs. 6(d,e).

The strong dependence of the current flowing across the left JJ by varying the phase difference across the right JJ signals the emergence of the nonlocal Josephson effect.

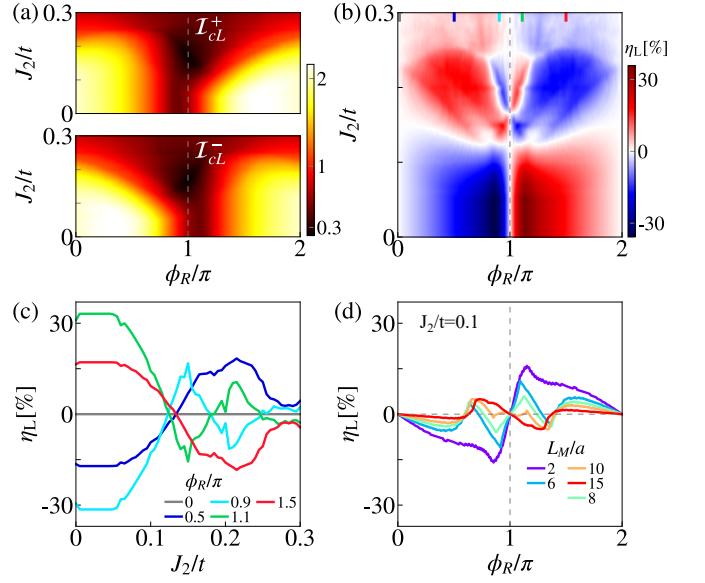


FIG. 3. (a) Critical currents  $\mathcal{I}_{cL}^{\pm}$  as a function of  $\phi_R$  and  $J_2$  under  $d_{x^2-y^2}$ -wave altermagnetism. (b) Quality factor  $\eta_L$  as a function of  $J_2$  and  $\phi_R$ . (c,d) Line cuts of (b) for distinct values of  $J_2$  and  $\phi_R$ . The values of  $\phi_R$  for the line cuts in (c) are marked by color bars in (b). Parameters:  $L_M = 2a$  and the rest is the same as in Fig. 1.

This effect in the left JJ is entirely determined by the spin-polarized Andreev molecules shown in Figs. 1(g,h), with current signals that can be directly tied to the respective energy branch. For instance, the large values of the current for  $\phi_L \in (0, \pi)$  and  $\phi_L \in (\pi, 2\pi)$  in JJs with  $d_{x^2-y^2}$ -wave altermagnetism is predominantly carried by Andreev molecules of one type of spin polarization within the gap, while outside it the opposite polarization also contributes [Fig. 1(h)]. In contrast, the arc surface region with smaller current intensities for  $\phi_L \in (\pi, 2\pi)$  corresponds to a regime where the Andreev molecules with distinct polarizations cross zero energy [Fig. 1(h)], leaving Andreev molecules with the same polarization but opposite contribution that end up cancelling out; thus, the values of the current in this case are dominated by the quasicontinuum. In a similar way, one can identify the contribution of spin-polarized Andreev molecules on the nonlocal Josephson effect in coupled JJs with  $d_{xy}$ -wave altermagnetism, see Figs. 6(b,c). We can therefore conclude that the formation of spin-polarized Andreev molecules enable the emergence of a nonlocal Josephson effect determining supercurrents with anomalous profiles.

*Nonlocal Josephson diode effect.*—The behavior of the nonlocal Josephson current  $\mathcal{I}_L(\phi_L, \phi_R)$  also reveals its nonreciprocity since the maximum and minimum currents are not equal  $\mathcal{I}_{cL}^+(\phi_R) \neq \mathcal{I}_{cL}^-(\phi_R)$ , where  $\mathcal{I}_{cL}^{\pm}(\phi_R) = \max_{\phi_L} [\pm \mathcal{I}_L(\phi_L, \phi_R)]$ . Using these definitions, in Fig. 3(a) we show  $\mathcal{I}_{cL}^{\pm}(\phi_R)$  as a function of  $J_2$  and  $\phi_R$  for a very short middle region  $L_M = 2a$  in the presence of  $d_{x^2-y^2}$ -wave altermagnetism. Fig. 3(a) shows that  $\mathcal{I}_{cL}^+(\phi_R) \neq$

$\mathcal{I}_{\text{CL}}^-(\phi_{\text{R}})$  for any  $\phi_{\text{R}}$  except  $\phi_{\text{R}} = n\pi$  with  $n \in \mathbb{Z}$ . The nonreciprocity in the nonlocal critical currents signal the emergence of the nonlocal Josephson diode effect. While  $\mathcal{I}_{\text{CL}}^{\pm}(\phi_{\text{R}})$  remain sizeable for  $J_2$  below  $\Delta$ , strong altermagnetic strengths tend to reduce the critical currents; in JJs with  $d_{x^2-y^2}$ -wave altermagnetism [Fig. 3(a)], the currents support stronger values of altermagnetic fields than in JJs with  $d_{xy}$ -wave AMs [Fig. 7(a)].

To assess the efficiency of the nonlocal Josephson diode effect, we obtain its quality factor as  $\eta_{\text{L}}(\phi_{\text{R}}) = [\mathcal{I}_{\text{CL}}^+(\phi_{\text{R}}) - \mathcal{I}_{\text{CL}}^-(\phi_{\text{R}})] / [\mathcal{I}_{\text{CL}}^+(\phi_{\text{R}}) + \mathcal{I}_{\text{CL}}^-(\phi_{\text{R}})]$  and show it in Fig. 3(b) as a function of  $J_2$  and  $\phi_{\text{R}}$  for JJs with  $d_{x^2-y^2}$ -wave altermagnetism, while in Fig. 6(b) for  $d_{xy}$ -wave AM case. The first observation is that  $\eta_{\text{L}}$  strongly depends on  $\phi_{\text{R}}$  as well as on the strength and type of altermagnetism. For  $\phi_{\text{R}} = n\pi$ , with  $n \in \mathbb{Z}$ , the quality factor vanishes since  $\mathcal{I}_{\text{CL}}^+ = \mathcal{I}_{\text{CL}}^-$ ; in this case, the Andreev spectrum is symmetric around  $\phi_{\text{L}} = \pi$ . Away from these phase values,  $\eta_{\text{L}}$  reach efficiencies of the order of 30% and notably develops an odd function dependence with  $\phi_{\text{R}}$  as a clear manifestation of the nonlocal Josephson effect; this also means that the diode's polarity  $\text{sgn}(\eta_{\text{L}})$  can be controlled nonlocally by  $\phi_{\text{R}}$ ; see Fig. 3(c) and Fig. 6(c). Furthermore, the diode's polarity can be controlled by the strength of altermagnetism, as demonstrated in Figs. 3(c,d) and Figs. 6(c,d) at fixed  $\phi_{\text{R}}$ . Under  $d_{x^2-y^2}$ -wave altermagnetism, changing the diode's polarity requires slightly stronger altermagnetic fields than under  $d_{xy}$ -wave altermagnetism but the former supports larger efficiencies at large fields. Nevertheless, in both types of AMs, reaching measurable nonlocal Josephson diode efficiencies requires the presence of spin-polarized Andreev molecules, which is only attained for short middle superconductors, as demonstrated in Fig. 3(d) and Fig. 6(d).

In conclusion, we have demonstrated the formation of spin-polarized Andreev molecules in weakly coupled Josephson junctions with zero net magnetization by utilizing altermagnetism. We showed that these spin-polarized Andreev molecules give rise to phase-biased nonlocal Josephson currents capable of developing  $\phi_0$ - and  $\pi$ -junction behaviors, which are tunable by the type and strength of altermagnetism. Moreover, we found that these nonlocal Josephson currents exhibit nonreciprocal critical currents, originating a nonlocal Josephson diode effect whose polarity is controllable nonlocally by the superconducting phase difference across the right Josephson junction as well as by the strength of altermagnetism. These predictions are applicable to higher angular momentum altermagnets, such as  $g$ - and  $i$ -wave, and offer a very likely nonlocal phase control of recently reported altermagnet-induced phenomena, such as exotic Cooper pairs [14, 96–108] and flat bands [109–111]. Our results establish altermagnetism as key ingredient for designing spin-polarized Andreev molecules and realizing anomalous Josephson states with nonlocal functionalities.

We acknowledge financial support from the Göran

Gustafsson Foundation (Grant No. 2216), from the Swedish Research Council (Vetenskapsrådet Grant No. 2021-04121), and from the Olle Engkvist Foundation (Grant No. 243-1026). The computations were enabled by resources provided by the National Academic Infrastructure for Supercomputing in Sweden (NAISS), partially funded by the Swedish Research Council through Grant Agreement No. 2022-06725.

- 
- [1] Y. Fukaya, B. Lu, K. Yada, Y. Tanaka, and J. Cayao, Superconducting phenomena in systems with unconventional magnets, *J. Phys.: Condens. Matter* **37**, 313003 (2025).
  - [2] Z. Liu, H. Hu, and X.-J. Liu, Altermagnetism and superconductivity: A short historical review, *arXiv*, 2510.09170 (2025).
  - [3] Y. Noda, K. Ohno, and S. Nakamura, Momentum-dependent band spin splitting in semiconducting mno 2: a density functional calculation, *Physical Chemistry Chemical Physics* **18**, 13294 (2016).
  - [4] M. Naka, S. Hayami, H. Kusunose, Y. Yanagi, Y. Motome, and H. Seo, Spin current generation in organic antiferromagnets, *Nat. Commun.* **10**, 4305 (2019).
  - [5] S. Hayami, Y. Yanagi, and H. Kusunose, Momentum-dependent spin splitting by collinear antiferromagnetic ordering, *J. Phys. Soc. Jpn.* **88**, 123702 (2019).
  - [6] K.-H. Ahn, A. Hariki, K.-W. Lee, and J. Kuneš, Antiferromagnetism in ruo<sub>2</sub> as  $d$ -wave Pomeranchuk instability, *Phys. Rev. B* **99**, 184432 (2019).
  - [7] L.-D. Yuan, Z. Wang, J.-W. Luo, E. I. Rashba, and A. Zunger, Giant momentum-dependent spin splitting in centrosymmetric low- $z$  antiferromagnets, *Phys. Rev. B* **102**, 014422 (2020).
  - [8] L. Šmejkal, R. González-Hernández, T. Jungwirth, and J. Sinova, Crystal time-reversal symmetry breaking and spontaneous Hall effect in collinear antiferromagnets, *Sci. Adv.* **6**, eaaz8809 (2020).
  - [9] M. Naka, S. Hayami, H. Kusunose, Y. Yanagi, Y. Motome, and H. Seo, Anomalous Hall effect in  $\kappa$ -type organic antiferromagnets, *Phys. Rev. B* **102**, 075112 (2020).
  - [10] L.-D. Yuan, Z. Wang, J.-W. Luo, and A. Zunger, Prediction of low- $z$  collinear and noncollinear antiferromagnetic compounds having momentum-dependent spin splitting even without spin-orbit coupling, *Phys. Rev. Mater.* **5**, 014409 (2021).
  - [11] L. Šmejkal, J. Sinova, and T. Jungwirth, Beyond conventional ferromagnetism and antiferromagnetism: A phase with nonrelativistic spin and crystal rotation symmetry, *Phys. Rev. X* **12**, 031042 (2022).
  - [12] I. Mazin (The PRX Editors), Editorial: Altermagnetism—a new punch line of fundamental magnetism, *Phys. Rev. X* **12**, 040002 (2022).
  - [13] L. Šmejkal, J. Sinova, and T. Jungwirth, Emerging research landscape of altermagnetism, *Phys. Rev. X* **12**, 040501 (2022).
  - [14] I. I. Mazin, Notes on altermagnetism and superconductivity, *AAPPS Bull.* **35**, 18 (2025).
  - [15] M. H. Devoret, A. Wallraff, and J. M. Martinis, Super-

- conducting qubits: A short review (2004), [arXiv:cond-mat/0411174 \[cond-mat.mes-hall\]](#).
- [16] J. Clarke and F. K. Wilhelm, Superconducting quantum bits, *Nature* **453**, 1031 (2008).
- [17] T. Brecht, W. Pfaff, C. Wang, Y. Chu, L. Frunzio, M. H. Devoret, and R. J. Schoelkopf, Multilayer microwave integrated quantum circuits for scalable quantum computing, *npj Quantum Inf.* **2**, 16002 (2016).
- [18] P. Krantz, M. Kjaergaard, F. Yan, T. P. Orlando, S. Gustavsson, and W. D. Oliver, A quantum engineer's guide to superconducting qubits, *Appl. Phys. Rev.* **6**, 021318 (2019).
- [19] J. M. Martinis, M. H. Devoret, and J. Clarke, Quantum Josephson junction circuits and the dawn of artificial atoms, *Nat. Phys.* **16**, 234 (2020).
- [20] R. Aguado, A perspective on semiconductor-based superconducting qubits, *Appl. Phys. Lett.* **117**, 240501 (2020).
- [21] M. Benito and G. Burkard, Hybrid superconductor-semiconductor systems for quantum technology, *Appl. Phys. Lett.* **116**, 190502 (2020).
- [22] R. Aguado and L. P. Kouwenhoven, Majorana qubits for topological quantum computing, *Phys. Today* **73**, 44 (2020).
- [23] J. Cayao, C. Triola, and A. M. Black-Schaffer, Odd-frequency superconducting pairing in one-dimensional systems, *Eur. Phys. J. Special Topics* **229**, 545 (2020).
- [24] S. Rasmussen, K. Christensen, S. Pedersen, L. Kristensen, T. Bækkegaard, N. Loft, and N. Zinner, Superconducting circuit companion—an introduction with worked examples, *PRX Quantum* **2**, 040204 (2021).
- [25] I. Siddiqi, Engineering high-coherence superconducting qubits, *Nat. Rev. Mater.* **6**, 875 (2021).
- [26] A. Bargerbos, M. Pita-Vidal, R. Žitko, J. Ávila, L. J. Splitthoff, L. Grünhaupt, J. J. Wesdorp, C. K. Andersen, Y. Liu, L. P. Kouwenhoven, R. Aguado, A. Kou, and B. van Heck, Singlet-doublet transitions of a quantum dot Josephson junction detected in a transmon circuit, *PRX Quantum* **3**, 030311 (2022).
- [27] M. Kjaergaard, M. E. Schwartz, J. Braumüller, P. Krantz, J. I.-J. Wang, S. Gustavsson, and W. D. Oliver, Superconducting qubits: Current state of play, *Annu. Rev. Condens. Matter Phys.* **11**, 369 (2020).
- [28] M. Pita-Vidal, A. Bargerbos, R. Žitko, L. J. Splitthoff, L. Grünhaupt, J. J. Wesdorp, Y. Liu, L. P. Kouwenhoven, R. Aguado, B. van Heck, *et al.*, Direct manipulation of a superconducting spin qubit strongly coupled to a transmon qubit, *Nat. Phys.* **19**, 1110 (2023).
- [29] Y. Tanaka, S. Tamura, and J. Cayao, Theory of Majorana zero modes in unconventional superconductors, *Prog. Theor. Exp. Phys.* **2024**, 08C105 (2024).
- [30] J. A. Ouassou, A. Brataas, and J. Linder, dc Josephson effect in altermagnets, *Phys. Rev. Lett.* **131**, 076003 (2023).
- [31] C. W. J. Beenakker and T. Vakhel, Phase-shifted Andreev levels in an altermagnet Josephson junction, *Phys. Rev. B* **108**, 075425 (2023).
- [32] Y. Fukaya, K. Maeda, K. Yada, J. Cayao, Y. Tanaka, and B. Lu, Josephson effect and odd-frequency pairing in superconducting junctions with unconventional magnets, *Phys. Rev. B* **111**, 064502 (2025).
- [33] S. Vosoughi-nia and M. P. Nowak, Altermon: a magnetic-field-free parity protected qubit based on a narrow altermagnet Josephson junction, [arXiv:2510.18145 \(2025\)](#).
- [34] S.-B. Zhang, L.-H. Hu, and T. Neupert, Finite-momentum Cooper pairing in proximitized altermagnets, *Nat. Commun.* **15**, 1801 (2024).
- [35] B. Lu, K. Maeda, H. Ito, K. Yada, and Y. Tanaka,  $\varphi$  Josephson junction induced by altermagnetism, *Phys. Rev. Lett.* **133**, 226002 (2024).
- [36] Q. Cheng and Q.-F. Sun, Orientation-dependent Josephson effect in spin-singlet superconductor/altermagnet/spin-triplet superconductor junctions, *Phys. Rev. B* **109**, 024517 (2024).
- [37] H.-P. Sun, S.-B. Zhang, C.-A. Li, and B. Trauzettel, Tunable second harmonic in altermagnetic Josephson junctions, *Phys. Rev. B* **111**, 165406 (2025).
- [38] W. Zhao, Y. Fukaya, P. Buset, J. Cayao, Y. Tanaka, and B. Lu, Orientation-dependent transport in junctions formed by  $d$ -wave altermagnets and  $d$ -wave superconductors, *Phys. Rev. B* **111**, 184515 (2025).
- [39] M. Alipourzadeh and Y. Hajati, Andreev bound states and supercurrent in an unconventional superconductor-altermagnet Josephson junction, *Phys. Rev. B* **111**, 214515 (2025).
- [40] A. Pal, D. Mondal, T. Nag, and A. Saha, Josephson current signature of Floquet Majorana and topological accidental zero modes in altermagnet heterostructures, *Phys. Rev. B* **112**, L201408 (2025).
- [41] Q. Cheng, Y. Mao, and Q.-F. Sun, Field-free Josephson diode effect in altermagnet/normal metal/altermagnet junctions, *Phys. Rev. B* **110**, 014518 (2024).
- [42] Y. Jiang, H.-L. Liu, and J. Wang, Josephson diode effect in altermagnet-based  $s$ -wave superconductor junction, *Chinese Phys. B* **34**, 107803 (2025).
- [43] L. Sharma and M. Thakurathi, Tunable Josephson diode effect in singlet superconductor-altermagnet-triplet superconductor junctions, *Phys. Rev. B* **112**, 104506 (2025).
- [44] D. Debnath, A. Saha, and P. Dutta, Spin-polarization and diode effect in thermoelectric current through altermagnet-based superconductor heterostructures, [arXiv:2509.12198 \(2025\)](#).
- [45] L. Sharma, B. Ghimire, and M. Thakurathi,  $p$ -wave magnet driven field-free Josephson diode effect, [arXiv:2602.16677 \(2026\)](#).
- [46] V. D. Esin, D. Y. Kazmin, Y. S. Barash, A. V. Timonina, N. N. Kolesnikov, and E. V. Deviatov, Josephson diode and spin-valve effects on the surface of altermagnet crsb, [arXiv:2602.08766 \(2026\)](#).
- [47] D. Shaffer and A. Levchenko, Theories of superconducting diode effects, [arXiv:2510.25864 \(2025\)](#).
- [48] J.-D. Pillet, V. Benzoni, J. Griesmar, J.-L. Smirr, and c. O. Girit, Nonlocal Josephson effect in Andreev molecules, *Nano Lett.* **19**, 7138 (2019).
- [49] J.-D. Pillet, V. Benzoni, J. Griesmar, J.-L. Smirr, and Çağlar Ö. Girit, Scattering description of Andreev molecules, *SciPost Phys. Core* **2**, 009 (2020).
- [50] H.-Y. Xie, M. G. Vavilov, and A. Levchenko, Weyl nodes in Andreev spectra of multiterminal Josephson junctions: Chern numbers, conductances, and supercurrents, *Phys. Rev. B* **97**, 035443 (2018).
- [51] R. Mélin, Inversion in a four-terminal superconducting device on the quartet line. i. two-dimensional metal and the quartet beam splitter, *Phys. Rev. B* **102**, 245435

- (2020).
- [52] R. Mélin, Ultralong-distance quantum correlations in three-terminal Josephson junctions, *Phys. Rev. B* **104**, 075402 (2021).
- [53] E. W. Hodt and J. Linder, On-off switch and sign change for a nonlocal Josephson diode in spin-valve Andreev molecules, *Phys. Rev. B* **108**, 174502 (2023).
- [54] J. Cayao, P. Burset, and Y. Tanaka, Controllable odd-frequency Cooper pairs in multiterminal superconductor Josephson junctions, *Phys. Rev. B* **109**, 205406 (2024).
- [55] J.-D. Pillet, S. Annabi, A. Peugeot, H. Riechert, E. Arrighi, J. Griesmar, and L. Bretheau, Josephson diode effect in Andreev molecules, *Phys. Rev. Res.* **5**, 033199 (2023).
- [56] F. Matute-Cañadas, L. Tosi, and A. L. Yeyati, Quantum circuits with multiterminal Josephson-Andreev junctions, *PRX Quantum* **5**, 020340 (2024).
- [57] M. Kocsis, Z. Scherübl, G. m. H. Fülöp, P. Makk, and S. Csonka, Strong nonlocal tuning of the current-phase relation of a quantum dot based Andreev molecule, *Phys. Rev. B* **109**, 245133 (2024).
- [58] J. Cayao and M. Sato, Non-Hermitian multiterminal phase-biased Josephson junctions, *Phys. Rev. B* **110**, 235426 (2024).
- [59] J. H. Correa and M. P. Nowak, Theory of universal diode effect in three-terminal Josephson junctions, *SciPost Phys.* **17**, 037 (2024).
- [60] P. Kotetes, M. Roig, and B. M. Andersen, Nonreciprocal equilibrium  $4\pi$ -periodic Josephson effect from poor man's Majorana zero modes, [arXiv:2409.13027](https://arxiv.org/abs/2409.13027) (2024).
- [61] G. A. Bobkov, D. S. Rabinovich, A. M. Bobkov, and I. V. Bobkova, Gate-tunable nonlocal Josephson effect through magnetic van der Waals bilayers, *Phys. Rev. B* **111**, 024506 (2025).
- [62] J. Cayao and M. Sato, Nonlocal Josephson diode effect in minimal Kitaev chains, [arXiv:2512.00664](https://arxiv.org/abs/2512.00664) (2025).
- [63] E. Strambini, S. D'ambrosio, F. Vischi, F. Bergeret, Y. V. Nazarov, and F. Giazotto, The  $\omega$ -squeezing as a tool to phase-engineer Josephson topological materials, *Nat. Nanotech.* **11**, 1055 (2016).
- [64] Z. Su, A. B. Tacla, M. Hocevar, D. Car, S. R. Plissard, E. P. A. M. Bakkers, A. J. Daley, D. Pekker, and S. M. Frolov, Andreev molecules in semiconductor nanowire double quantum dots, *Nat. Commun.* **8**, 585 (2017).
- [65] A. W. Draelos, M.-T. Wei, A. Seredinski, H. Li, Y. Mehta, K. Watanabe, T. Taniguchi, I. V. Borzenets, F. Amet, and G. Finkelstein, Supercurrent flow in multi-terminal graphene Josephson junctions, *Nano Lett.* **19**, 1039 (2019).
- [66] N. Pankratova, H. Lee, R. Kuzmin, K. Wickramasinghe, W. Mayer, J. Yuan, M. G. Vavilov, J. Shabani, and V. E. Manucharyan, Multiterminal Josephson effect, *Phys. Rev. X* **10**, 031051 (2020).
- [67] G. V. Graziano, M. Gupta, M. Pendharkar, J. T. Dong, C. P. Dempsey, C. Palmström, and V. S. Pribiag, Selective control of conductance modes in multi-terminal Josephson junctions, *Nat. Commun.* **13**, 5933 (2022).
- [68] S. Matsuo, J. S. Lee, C.-Y. Chang, Y. Sato, K. Ueda, C. J. Palmström, and S. Tarucha, Observation of non-local Josephson effect on double InAs nanowires, *Commun. Phys.* **5**, 221 (2022).
- [69] C. Jünger, S. Lehmann, K. A. Dick, C. Thelander, C. Schönenberger, and A. Baumgartner, Intermediate states in Andreev bound state fusion, *Communications Physics* **6**, 190 (2023).
- [70] S. Matsuo, T. Imoto, T. Yokoyama, Y. Sato, T. Lindemann, S. Gronin, G. C. Gardner, M. J. Manfra, and S. Tarucha, Phase engineering of anomalous Josephson effect derived from Andreev molecules, *Sci. Adv.* **9**, eadj3698 (2023).
- [71] S. Matsuo, T. Imoto, T. Yokoyama, Y. Sato, T. Lindemann, S. Gronin, G. C. Gardner, S. Nakosai, Y. Tanaka, M. J. Manfra, *et al.*, Phase-dependent Andreev molecules and superconducting gap closing in coherently-coupled Josephson junctions, *Nat. Commun.* **14**, 8271 (2023).
- [72] D. Z. Haxell, M. Coraiola, M. Hinderling, S. C. ten Kate, D. Sabonis, A. E. Svetogorov, W. Belzig, E. Cheah, F. Krizek, R. Schott, W. Wegscheider, and F. Nichele, Demonstration of the nonlocal Josephson effect in Andreev molecules, *Nano Lett.* **23**, 7532 (2023).
- [73] D. van Driel, B. Roovers, F. Zatelli, A. Bordin, G. Wang, N. van Loo, J. C. Wolff, G. P. Mazur, S. Gazibegovic, G. Badawy, E. P. Bakkers, L. P. Kouwenhoven, and T. Dvir, Charge sensing the parity of an Andreev molecule, *PRX Quantum* **5**, 020301 (2024).
- [74] S. Zhu, Y. Ma, J. He, X. Yang, Z. Jia, M. Wei, Y. Jiao, J. He, E. Zhuo, X. Cao, *et al.*, Josephson diode effect in nanowire-based Andreev molecules, *Commun. Phys.* **8**, 330 (2025).
- [75] J. Hu, C. Wu, and X. Dai, Proposed design of a Josephson diode, *Phys. Rev. Lett.* **99**, 067004 (2007).
- [76] F. Dolcini, M. Houzet, and J. S. Meyer, Topological Josephson  $\phi_0$  junctions, *Phys. Rev. B* **92**, 035428 (2015).
- [77] K. N. Nesterov, M. Houzet, and J. S. Meyer, Anomalous Josephson effect in semiconducting nanowires as a signature of the topologically nontrivial phase, *Phys. Rev. B* **93**, 174502 (2016).
- [78] K. Misaki and N. Nagaosa, Theory of the nonreciprocal Josephson effect, *Phys. Rev. B* **103**, 245302 (2021).
- [79] Y. Tanaka, B. Lu, and N. Nagaosa, Theory of giant diode effect in  $d$ -wave superconductor junctions on the surface of a topological insulator, *Phys. Rev. B* **106**, 214524 (2022).
- [80] M. Davydova, S. Prembabu, and L. Fu, Universal Josephson diode effect, *Sci. Adv.* **8**, eabo0309 (2022).
- [81] S. Mondal, P.-H. Fu, and J. Cayao, Josephson diode effect with Andreev and Majorana bound states, *Phys. Rev. B* **112**, 144506 (2025).
- [82] J. Cayao, N. Nagaosa, and Y. Tanaka, Enhancing the Josephson diode effect with Majorana bound states, *Phys. Rev. B* **109**, L081405 (2024).
- [83] R. Seoane Souto, M. Leijnse, C. Schrade, M. Valentini, G. Katsaros, and J. Danon, Tuning the Josephson diode response with an ac current, *Phys. Rev. Res.* **6**, L022002 (2024).
- [84] Z. Liu, L. Huang, and J. Wang, Josephson diode effect in topological superconductors, *Phys. Rev. B* **110**, 014519 (2024).
- [85] Y. Zhang, Y. Gu, P. Li, J. Hu, and K. Jiang, General theory of Josephson diodes, *Phys. Rev. X* **12**, 041013 (2022).
- [86] C. Beenakker, Three “universal” mesoscopic Josephson effects, in *Transport phenomena in mesoscopic systems: Proceedings of the 14th Taniguchi symposium, Shima, Japan, November 10-14, 1991*, Vol. 109 (Springer-Verlag, Berlin, 1992) p. 235.
- [87] A. Zagoskin, *Quantum Theory of Many-Body Systems:*

*Techniques and Applications* (Springer, Berlin, 2014).

- [88] A. Furusaki and M. Tsukada, Dc Josephson effect and Andreev reflection, *Solid State Commun.* **78**, 299 (1991).
- [89] A. Furusaki, Josephson current carried by Andreev levels in superconducting quantum point contacts, *Superlattices and Microstructures* **25**, 809 (1999).
- [90] S. Kashiwaya and Y. Tanaka, Tunnelling effects on surface bound states in unconventional superconductors, *Rep. Prog. Phys.* **63**, 1641 (2000).
- [91] J. Cayao, P. San-Jose, A. M. Black-Schaffer, R. Aguado, and E. Prada, Majorana splitting from critical currents in Josephson junctions, *Phys. Rev. B* **96**, 205425 (2017).
- [92] J. Cayao, A. M. Black-Schaffer, E. Prada, and R. Aguado, Andreev spectrum and supercurrents in nanowire-based SNS junctions containing Majorana bound states, *Beilstein J. Nanotechnol.* **9**, 1339 (2018).
- [93] O. A. Awoga, J. Cayao, and A. M. Black-Schaffer, Supercurrent detection of topologically trivial zero-energy states in nanowire junctions, *Phys. Rev. Lett.* **123**, 117001 (2019).
- [94] J. Cayao and A. M. Black-Schaffer, Distinguishing trivial and topological zero-energy states in long nanowire junctions, *Phys. Rev. B* **104**, L020501 (2021).
- [95] A. A. Golubov, M. Y. Kupriyanov, and E. Il'ichev, The current-phase relation in Josephson junctions, *Rev. Mod. Phys.* **76**, 411 (2004).
- [96] K. Maeda, Y. Fukaya, K. Yada, B. Lu, Y. Tanaka, and J. Cayao, Classification of pair symmetries in superconductors with unconventional magnetism, *Phys. Rev. B* **111**, 144508 (2025).
- [97] D. Chakraborty and A. M. Black-Schaffer, Constraints on superconducting pairing in altermagnets, *Phys. Rev. B* **112**, 014516 (2025).
- [98] M. Khodas, S. Mu, I. I. Mazin, and K. D. Belashchenko, Tuning of altermagnetism by strain, [arXiv:2506.06257](https://arxiv.org/abs/2506.06257) (2025).
- [99] X. Feng and Z. Zhang, Superconducting order parameters in spin space groups: Methodology and application, *Phys. Rev. B* **111**, 054520 (2025).
- [100] K. Parshukov and A. P. Schnyder, Exotic superconducting states in altermagnets, [arXiv:2507.10700](https://arxiv.org/abs/2507.10700) (2025).
- [101] P.-H. Fu, S. Mondal, J.-F. Liu, and J. Cayao, Light-induced Floquet spin-triplet Cooper pairs in unconventional magnets, *SciPost Phys.* **20**, 059 (2026).
- [102] P.-H. Fu, S. Mondal, J.-F. Liu, Y. Tanaka, and J. Cayao, Floquet engineering spin triplet states in unconventional magnets, *Phys. Rev. Lett.* **136**, 066703 (2026).
- [103] T. Yokoyama, Floquet engineering triplet superconductivity in superconductors with spin-orbit coupling or altermagnetism, *Phys. Rev. B* **112**, 024512 (2025).
- [104] K. Mukasa and Y. Masaki, Finite-momentum superconductivity in two-dimensional altermagnets with a Rashba-type spin-orbit coupling, *J. Phys. Soc. Jpn.* **94**, 064705 (2025).
- [105] N. Heinsdorf and M. Franz, Proximitizing altermagnets with conventional superconductors, [arXiv:2509.03774](https://arxiv.org/abs/2509.03774) (2025).
- [106] K. Monkman, J. Weng, N. Heinsdorf, A. Nocera, and M. Franz, Persistent spin currents in superconducting altermagnets, [arXiv:2507.22139](https://arxiv.org/abs/2507.22139) (2025).
- [107] J. Chang, H. Lu, J. Zhao, H.-G. Luo, and Y. Ding, Energy dispersion, superconductivity, and magnetic fluctuations in stacked altermagnetic materials, *Phys. Rev. B* **111**, 104432 (2025).
- [108] M. Khodas, L. Šmejkal, and I. I. Mazin, Nonrelativisticising superconductivity in  $p$ -wave magnets, [arXiv:2601.19829](https://arxiv.org/abs/2601.19829) (2026).
- [109] B. Lu, P. Mercebach, P. Bursset, K. Yada, J. Cayao, Y. Tanaka, and Y. Fukaya, Engineering subgap states in superconductors by altermagnetism, [arXiv: 2508.03364](https://arxiv.org/abs/2508.03364) (2025).
- [110] Z. Liu, H. Hu, and X. Ji Liu, Fulde-Ferrell-Larkin-Ovchinnikov states and topological Bogoliubov Fermi surfaces in altermagnets: an analytical study, [arXiv: 2508.07813](https://arxiv.org/abs/2508.07813) (2025).
- [111] Y. Fukaya, B. Lu, K. Yada, Y. Tanaka, and J. Cayao, Crossed surface flat bands in three-dimensional superconducting altermagnets, [arXiv:2510.14724](https://arxiv.org/abs/2510.14724) (2026).

## END MATTER

*E1. Localization of Andreev molecules.*—The hybridization of spin-polarized ABSs in the JJ setup of Fig. 1(a) is due to the reduced length of the middle superconductor, which leads to a strong coupling between left and right JJs. To see the real space behavior of such hybridization, Fig. 4 shows the space dependence of the wave function probability density of the first positive state for  $L_M = 100a$  and  $L_M = 2a$  for distinct  $\phi_{L,R}$ . When  $L_M = 100a$ , the coupling between left and right JJs is very weak, such that the ABSs localized at each JJ do not hybridize [Fig. 4(a)]: as seen, the ABSs are strongly localized at each JJ, with their wavefunctions decaying towards the bulk of the middle superconductor that depends on  $k_y$  but without developing any spatial overlap. In contrast, for  $L_M = 2a$ , the wavefunctions of the ABSs of the left and right JJs strongly hybridize, with a profile that resembles that of an ABS localized at a single interface. The wavefunction profile of this spin-polarized Andreev molecule depends on  $k_y$  and  $\phi_{L,R}$ , which can influence the decay itself and its oscillations.

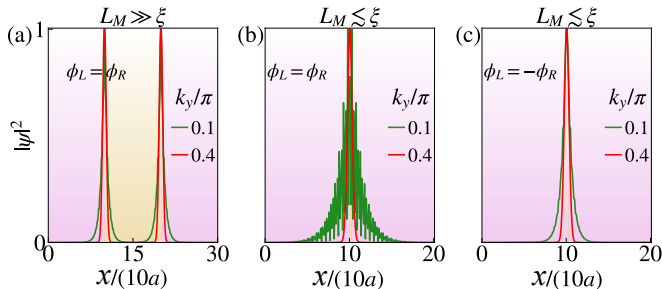


FIG. 4. Wave function probability density of the first positive state for a JJ with  $d_{x^2-y^2}$ -wave altermagnetism as a function of space for  $L_M = 100a$  (a) and  $L_M = 2a$  (b,c), in both cases with  $\phi_R = 0.7\pi$ . The green and the red curves indicate two different values of  $k_y$ . Parameters:  $J_1 = 0$ ,  $J_2 = 0.1t$ ; the rest is the same as in Fig. 1.

*E2. Molecular behavior of the hybridized Andreev states.*—The molecular nature of the spin-polarized ABSs can be directly seen in the dependence of the energy levels on  $L_M$ , presented in Fig. 5 at  $\phi_L = 0.7\pi = \phi_R$  and  $\phi_L = 1.3\pi \neq \phi_R$  for altermagnetic strengths corresponding to Fig. 1. Without AMs, the energy levels are spin degenerate but already here the levels develop an interesting behavior with  $L_M$ , see Fig. 5(a): at long  $L_M$ , each JJ hosts ABSs which are degenerate but begin to split at  $L_M \sim 50a$ , followed by a behavior that depends on  $\phi_{L,R}$ . For  $\phi_L = 1.3\pi \neq \phi_R$ , the energy levels below  $L_M \sim 50a$  form bonding and antibonding molecular states, with a clear minimum and an overall energy dependence that resembles the interatomic potential describing molecular formation [Fig. 5(a)]. For  $\phi_L = 0.7\pi = \phi_R$ , the splitting between ABSs induced by the hybridization is weaker

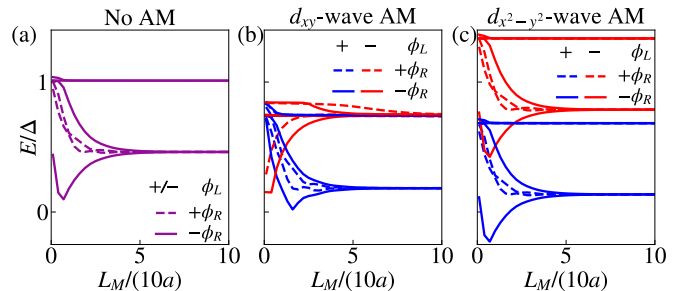


FIG. 5. Lowest four positive levels of each  $\pm$  sector as a function of  $L_M$  in the absence (a) and presence of altermagnetism (b,c) at  $\phi_R = 0.7\pi$ ,  $k_y = 0.1\pi$ . The dashed and solid curves correspond to  $\phi_L = 0.7\pi = \phi_R$  and  $\phi_L = 1.3\pi = -\phi_R$  respectively. Parameters:  $J_{1,2} = 0$  in (a),  $J_1 = 0.1t$  and  $J_2 = 0$  in (b),  $J_1 = 0$  and  $J_2 = 0.1t$  in (c), and the rest as in Fig. 1.

below  $L_M \sim 50a$ , ultimately pushing both levels into the quasicontinuum. Interestingly, in the presence of altermagnetism, ABSs are split in spin and, interestingly, such spin-polarized ABSs still develop the molecular formation profile for  $\phi_L = 1.3\pi \neq \phi_R$  and in both types of altermagnetism, see Figs. 5(b,c). This demonstrates the emergence of spin-polarized Andreev molecules.

*E4. Nonlocal Josephson effect in junctions with  $d_{xy}$ -wave altermagnetism.*—In the case of  $d_{xy}$ -wave altermagnetism, the total Josephson current flowing across the left JJ  $\mathcal{I}_L(\phi_L, \phi_R)$  is presented in Figs. 6(a,b) as a function of  $\phi_{L,R}$  for long ( $L_M \gg \xi$ ) and short ( $L_M \lesssim \xi$ ) middle superconductors at  $J_1/t = 0.1$ . Fig. 6(c) shows  $\mathcal{I}_L(\phi_L, \phi_R)$  versus  $\phi_{L,R}$  for  $J_1/t = 0.3$ , while Figs. 6(d,e) shows line cuts of Fig. 6(b) as a function of  $\phi_{L,R}$  at distinct  $\phi_{R,L}$ . For  $L_M \gg \xi$ , Fig. 6(a) reveals that  $\mathcal{I}_L(\phi_L, \phi_R)$  is an odd function of  $\phi_R$  but independent of  $\phi_L$ ; this is because the left and right JJs are effectively uncoupled (very weakly coupled) and the spin-polarized ABSs in each JJ do not hybridize. When  $L_M \lesssim \xi$ ,  $\mathcal{I}_L(\phi_L, \phi_R)$  exhibits large intensities that strongly dependent on both  $\phi_{L,R}$  and  $J_1$ , see Fig. 6(b-d). First of all,  $\mathcal{I}_L(\phi_L, \phi_R)$  is an odd function under both  $\phi_{L,R}$  and develops nonzero values at  $\phi_L = n\pi$  for  $\phi_R \neq n\pi$  [Fig. 6(b)], similar to JJs with  $d_{x^2-y^2}$ -wave altermagnetism shown in Figs. 2(b,d,e). As a result, the current across the left JJ can develop  $\phi_{L0}$ -junction behavior as a function of  $\phi_{L,R}$  but  $\pi$  behavior only as a function of  $\phi_R$  [Figs. 2(b,d,e)], hence establishing similarities and differences with respect to JJs with  $d_{x^2-y^2}$ -wave altermagnetism. The different behaviors can be controlled by the strength of  $d_{xy}$ -wave altermagnetism [Fig. 2(c)].

The intriguing behavior of the anomalous Josephson current  $\mathcal{I}_L(\phi_L, \phi_R)$  discussed above can be directly traced back to the behavior of the spin-polarized Andreev molecules shown in Fig. 1(g). For instance, for  $\phi_R = 0.7\pi$  in Fig. 1(g), the Andreev molecules inside the gap with

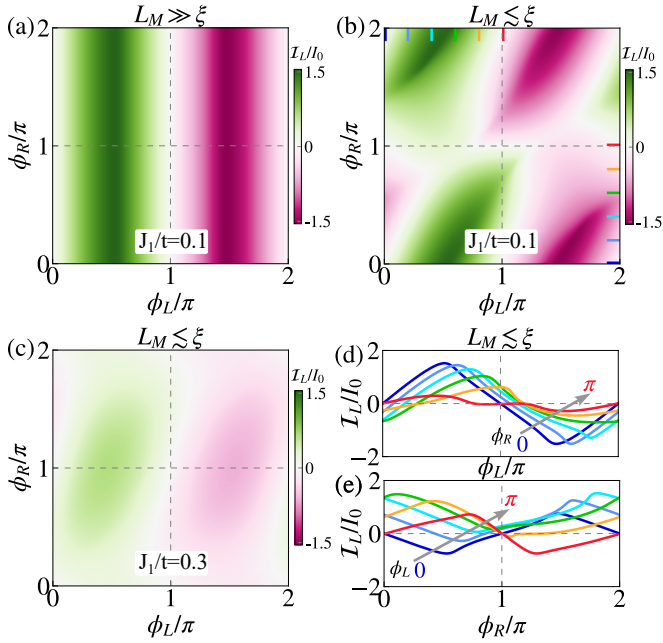


FIG. 6. The Josephson current  $\mathcal{I}_L$  across the left JJ as a function of  $\phi_{L,R}$  in the presence of  $d_{xy}$ -wave altermagnetism. (a)  $\mathcal{I}_L$  for  $L_M = 100a \gg \xi$  and  $J_1/t = 0.1$ , while (b,c) for  $L_M = 2a \lesssim \xi$  and  $J_1/t = \{0.1, 0.3\}$ . (d,e) Line cuts of  $\mathcal{I}_L$  in (b) as a function of  $\phi_{L(R)}$  at distinct  $\phi_{R(L)}$  in steps of  $0.2\pi$  marked by color bars in (b). Parameters same as in Fig. 1

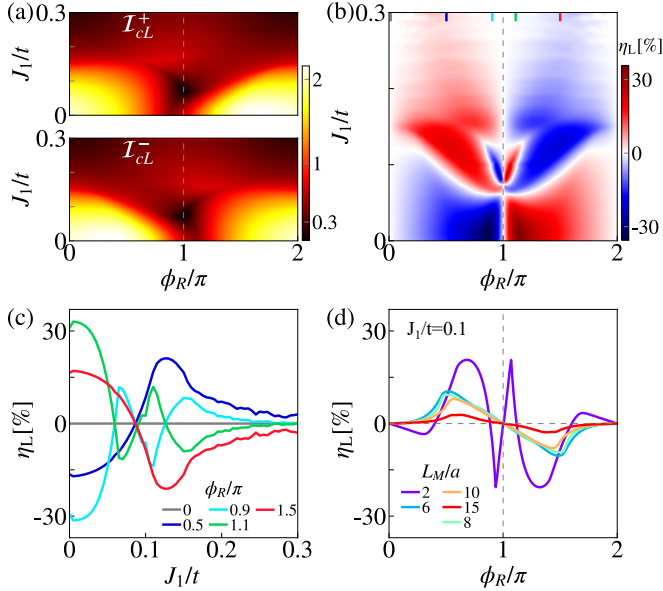


FIG. 7. (a) Critical currents  $\mathcal{I}_{cL}^{\pm}$  as a function of  $\phi_R$  and  $J_1$  under  $d_{xy}$ -wave altermagnetism. (b) Quality factor  $\eta_L$  as a function of  $J_1$  and  $\phi_R$ . (c,d) Line cuts of (b) for distinct values of  $J_1$  and  $\phi_R$ . The values of  $\phi_R$  for the line cuts in (c) are marked by color bars in (b). Parameters:  $L_M = 2a$  and the rest is the same as in Fig. 1.

positive spin polarization produce a negative supercurrent roughly below  $\phi_L < 0.7$ , while above such a phase, the Andreev molecule with opposite polarization domi-

nates and gives a positive supercurrent [Fig. 6(b)]; this explains the transition from a red-to-green color in the intensities of the current in Fig. 6(b), see also region between orange and green horizontal markers in Fig. 6(b). The absence of a  $\pi$ -junction behavior as a function of  $\phi_L$  can be also explained with the behavior of the Andreev molecules: Andreev molecules with both polarizations always share the contribution within the gap and  $\phi_L \in (0, 2\pi)$  since  $d_{xy}$ -wave altermagnetism shifts the subgap levels only in  $\phi_L$ . This makes it challenging to accommodate a single Andreev molecule giving a negative current for JJs with  $d_{xy}$ -wave altermagnetism. This is different to what occurs in  $d_{x^2-y^2}$ -wave altermagnetism [Figs. 2(b,d)] since therein the altermagnetic field shifts the energy levels in energy, which can leave a single Andreev molecule with a phase dependence supporting a  $\pi$ -junction. In sum, the nonlocal Josephson currents across the left JJ under  $d_{xy}$ -wave altermagnetism can develop  $\phi_{L0}$ - and  $\pi$ -junction behaviors controlled by the superconducting phases and altermagnetic strength.

*E5. Nonlocal Josephson diode effect in junctions with  $d_{xy}$ -wave altermagnetism.*—The anomalous nonlocal Josephson currents flowing across the left junction of Fig. 6 also exhibit regimes with distinct critical currents  $\mathcal{I}_{cL}^+(\phi_R) \neq \mathcal{I}_{cL}^-(\phi_R)$ , hence leading to a nonlocal Josephson diode effect under  $d_{xy}$ -wave altermagnetism characterized by a nonzero quality factor  $\eta_L(\phi_R) \neq 0$ . To understand this behavior, in Figs. 7(a,b) we present  $\mathcal{I}_{cL}^{\pm}(\phi_R)$  and  $\eta_L(\phi_R)$  as functions of  $\phi_R$  and  $J_1$  for a short middle superconductor ( $L_M \lesssim \xi$ ); in Figs. 7(c,d) we further show  $\eta_L(\phi_R)$  as a function of  $J_1$  for distinct  $\phi_R$  and as a function of  $\phi_R$  for different values of  $L_M$ . First, the critical currents  $\mathcal{I}_{cL}^{\pm}(\phi_R)$  exhibit values that do not follow the same dependence as a function of  $\phi_R$  and  $J_1$ , and with a particular asymmetric profile about  $\phi_R = \pi$ , see Fig. 7(a). By acquiring distinct values, the critical currents become nonreciprocal and signal the emergence of a nonlocal Josephson diode effect in coupled JJs with  $d_{xy}$ -wave altermagnetism. This diode effect is characterized by a finite quality factor  $\eta_L$  in Fig. 7(b), which acquires an odd function dependence in  $\phi_R$  that serves as a knob to control the diode's polarity. Notably, the nonlocal diode's polarity can be also controlled by the strength of  $d_{xy}$ -wave altermagnetism, which can be seen by noting the change in the sign of  $\eta_L$  with  $J_1$  in Fig. 7(b); see also Fig. 7(c). This implies that  $d_{xy}$ -wave altermagnetism acts a switcher to turn on and off the nonlocal Josephson diode effect, in the same way as  $d_{x^2-y^2}$ -wave altermagnetism shown in Figs. 3(b,c). While there exist some similarities in how the diode's quality factor responds to both types of altermagnetic symmetries, the field strengths needed for manipulating the polarity is lower in coupled JJs with  $d_{xy}$ -wave altermagnetism, but larger efficiencies are supported with  $d_{x^2-y^2}$ -wave altermagnetism.